Original Article

http://dx.doi.org/10.4322/2176-1523.0770

CYCLIC OXIDATION OF FERRITIC STAINLESS STEEL AISI 409

Samara Clotildes Saraiva Rodrigues [1]
Diego Machado dos Santos [2]
Ayrton de Sá Brandim [1]
Maura Célia Cunha e Silva [2]
Vanessa de Freitas Cunha Lins [3]
Maria de Fátima Salgado [4]

Abstract

The purpose of this study is to investigate the kinetics of growth, microstructure and chemical composition of the oxide films formed on AISI 409 ferritic stainless steel stabilized with titanium, after the cyclic oxidation process at a temperature typical of muffler (300°C), component belonging to the cold exhaust of the automobiles, in synthetic air in a tube furnace under two different conditions: oxidation after immersing the steel in the synthetic condensed (TOC) for 10 h and oxidation without immersion in the synthetic condensed (TOP). The kinetics of growth of oxide films was established by measuring the mass gain per unit area versus time. The microstructure and chemical composition of the oxides were analyzed by scanning electron microscopy (SEM) and energy dispersive spectroscopy (EDS). EDS analysis of the films formed on the samples showed the main chemical elements: Fe, Ti, Cr, S and Si. The presence of chromium was identified in proportions indicating the formation of protective oxides, as a film of Cr_2O_3 in the sample used as control, while the test specimen immersed in condensed showed failure of the oxide film after the 120th oxidation cycle.
Keywords: Ferritic stainless steel AISI 409; Corrosion; Condensed; Cyclic oxidation.

OXIDAÇÃO CÍCLICA DE AÇO INOXIDÁVEL FERRÍTICO AISI 409

Resumo

O objetivo do presente estudo é investigar a cinética de crescimento, microestrutura e composição química dos filmes de óxidos formados sobre o aço inoxidável ferrítico AISI 409 estabilizado com titânio, após o processo de oxidação cíclica a temperatura típica do silenciador (300°C), componente pertencente à parte fria do escapamento de automóveis, em atmosfera de ar sintético, em forno tubular sob duas condições diferentes: oxidação após imersão do aço no condensado sintético (TOC) por 10 h, e oxidação sem imersão no condensado (TOP). A cinética de crescimento dos filmes foi estabelecida medindo-se o ganho de massa por unidade de área versus tempo. A microestrutura e a composição química dos óxidos foram analisadas por microscopia eletrônica de varredura (MEV) e espectroscopia de energia dispersiva (EDS). Análises de EDS dos filmes formados sobre as amostras mostraram como principais elementos químicos: Fe, Ti, Cr, S e Si. Foi constatada a presença de cromo, em proporções que sugerem a formação de óxidos protetores, como uma película de Cr_2O_3 na amostra que serviu de controle, ao passo que, o corpo de prova imerso no condensado apresentou ruptura do filme após o centésimo vigésimo ciclo de oxidação.
Palavras-chave: Aço inoxidável ferrítico AISI 409; Corrosão; Condensado; Oxidação cíclica.

1 INTRODUCTION

In literature, high temperature oxidation studies of ferritic stainless steels were found. Parameters such as oxygen partial pressure, chromium content in the alloy were evaluated, and aspects such as kinetic behavior, mechanism of the chromia formation, and selective oxidation were studied [1,2]. Recent study of the effect of the grain boundary on the oxidation resistance of ferritic stainless steel showed that coarse oxide forms at random boundaries, and coincident site lattice (CSL) boundaries are oxidation resistant [3]. New techniques such as room temperature photoelectrochemistry was used to characterize oxide phases grown during the initial stages of oxidation of the ferritic

[1] *Instituto Federal Institute do Piauí - IFPI, Teresina, PI, Brazil.*
[2] *Universidade Estadual do Maranhão - UEMA, Caxias, MA, Brazil.*
[3] *Universidade Federal de Minas Gerais - UFMG, Belo Horizonte, MG, Brazil.*
[4] *Universidade Estadual do Maranhão - UEMA, Caxias, MA, Brazil. E-mail: fatima.salgado@pq.cnpq.br*

stainless steel AISI 441 at 650°C and 850°C in synthetic air or in water vapor [4]. Important research was developed to study the metal/oxide interface at short high temperature oxidation duration and an oxidation model was proposed [5].

The exhaust system of the motor consists of two parts: the hot part composed mainly by the collector, front pipe and catalytic converter, which work at an average temperature above 750°C, and the cold end composed mainly of muffler and tip, and both operate in medium at a temperature below 750°C.

The condensation of the gases occurs in muffler. The problem with this part of the exhaust is precisely the consequence of the interaction of the condensate with the metal part of the muffler.

For each type of fuel, a specific condensate is produced but, in general, its initial pH is between 8 and 9. With successive stops of the vehicle, the condensate tends to become increasingly aggressive because of the accumulation of chloride ions and the decrease in pH, which becomes 3 by liquid evaporation. For Li et al. [6], the chloride and sulfate ions and the low pH are most responsible for the corrosion of the muffler, considering that the sulfur content in the fuel, pollution of the atmosphere and the rate of motion of the vehicle are also important factors which cause the corrosion of the muffler.

Cunto [7] performed cyclic oxidation tests on AISI 409 steel stabilized with titanium and niobium and showed that after 500 hours the steel had already points of yellowish corrosion on its surface, and as the time increased the presence of dark oxides on the surface of the specimen increased.

Li et al. [6] also promoted similar oxidation tests with AISI 409 steel stabilized with niobium and titanium, comparing samples with and without previous immersion in condensate at three different temperatures. After ten cycles, the species immersed in condensate showed corrosion, this process spread over the surface when the sample temperature ranged from 250°C to 400°C. The oxidation points were weakly visible at 300°C, but totally visible at 400°C.

The lack of stabilization in stainless steel causes the diffusion of interstitial elements to the grain boundaries thereby precipitating carbides ($Cr_{23}C_6$) and nitrides (Cr_2N). This formation causes depletion of chromium in the grain boundary [8]. The addition of stabilizers such as Nb and Ti contribute to reduce interstitial solid solution elements.

The cyclic oxidation behavior of AISI 409 ferritic steel immersed in condensate was evaluated and compared with the behavior of cyclic oxidation of the same steel without immersion in condensate, for 120 cycles, at 300°C under an atmosphere of synthetic air in a tubular oven.

Table 1. Chemical composition of steel (wt. %), except iron (obtained by mass balance)

C	Si	Mn	P	Cr	N	Ti
0.03	1.00	1.00	0.04	10.5 -11.7	0.03	6(C+N)‹Ti‹0.75

2 MATERIAL AND METHODS

The steel samples were provided by APERAM South America and their chemical composition is shown in Table 1. The ferritic stainless steel AISI 409 has up to 0.08% of carbon, which ensures good weldability, 10 to 12% of chromium, which provides a reasonable resistance to corrosion and titanium, the minimum quantity of 6 times the ratio of carbon, limited to 0.75%, which makes it stabilized [9]. AISI 409 steel with Ti monostabilized used in this study belongs to the second generation of ferritic stainless steels, alloys with lower levels of C and Cr.

The test samples were used in the form of plates with an area of 217.4 mm^2 (sample immersed in condensate) and of 218.4 mm^2 (sample oxidized without immersion). After sanding with silicon carbide with sandpapers of 1000 mesh and 1240 mesh, the samples were polished with suspensions of diamond with grain sizes of 1 and 3μm in an automatic polisher. The final cleaning of the samples was performed using acetone and LIMP-SONIC ultrasound equipment to remove all moisture, and the samples were subjected to air blasting.

The samples were submitted to cyclic oxidation with previous immersion in condensate (TOC), and without immersion in condensed solution (TOP). Table 2 shows the experimental procedure.

The synthetic condensed solution was prepared according to a chemical composition provided by the metallurgical company [10]. The chemical composition of the synthetic condensate was: 0.077 g of NH_4NO_3; 1.017 g of $(NH_4)_2SO_4$; 0.1345 g of KCl; 0.33 ml of NH_4OH; 5.8 mL of HCl 1M, the volume was completed with distilled water until 1 L. Reagents were used in analytical degree without prior purification.

Table 2. Experimental procedure

Test	TOC	TOP
1	60 cycles of immersion in condensed solution for 5 minutes and rest time in air for 5 minutes at 70°C	Rest time in air for 10 h
2	Mass measurement	Mass measurement
3	120 cycles of 2 hours: oxidation at 300°C for 1 h and rest time at room temperature for 1 hour	120 cycles of 2 hours: oxidation at 300°C for 1 h and rest time at room temperature for 1 hour
4	Mass measurement	Mass measurement

The sample TOC was immersed in condensed solution in 5 minutes cycles. The alternate immersion was performed at 70°C for 10 h.

For all oxidation tests, an atmosphere of synthetic air was used through the hot zone of the tubular oven (JUNG). The thermal cycle of the two samples was oxidation for one hour at 300°C, followed by a rest period at room temperature for 1 h. During each cycle (Dip-Dry), the mass gain was continuously measured using a Shimadzu electronic scale with a sensitivity of 0.0001 g.

The kinetic behavior was evaluated measuring the mass gain per area. One hundred and twenty cycles were performed, and each cycle had the duration of 2 hours, totalizing 240 hours for each sample.

The sample characterization was performed using the scanning electron microscopy (JEOL JSM - 6360LV) and dispersive energy spectroscopy.

3 RESULTS

The mass gain of the sample oxidized for 240 hours without previous immersion in condensed solution was 4.58 10^{-5} g.cm^{-2}, and the mass gain of the sample oxidized after immersion in condensed solution was 2.21 10^{-3} g.cm^{-2}.

After the 96° cycle, the sample oxidized after immersion in condensed solution showed yellowish iron oxides. Several craters were observed on the surface of oxidized samples after immersion in the condensate (Figure 1).

The protective oxide film consists of three layers (Figure 2a), and Figure 2b is highlighted the rupture of the inner layer.

The rupture of the oxide film occurred preferentially in the region of the grain boundaries (Figure 3a). Figure 3b shows crevices among the grains, at the region of grain boundaries.

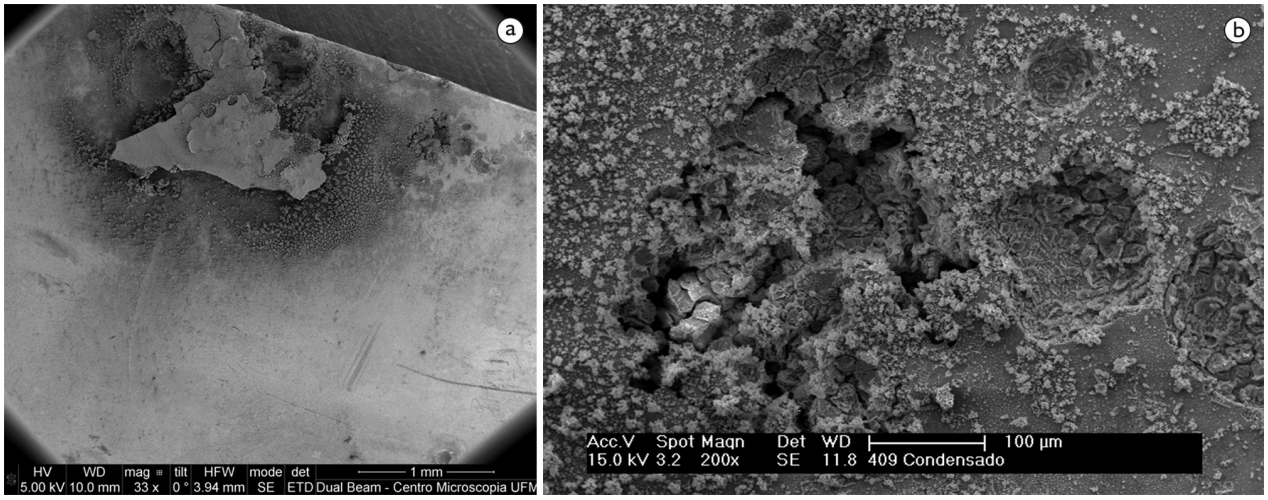

Figure 1. (a) Micrograph of the surface of oxidized steel after immersion in the condensate after the 120th oxidation cycle (b) Corroded area

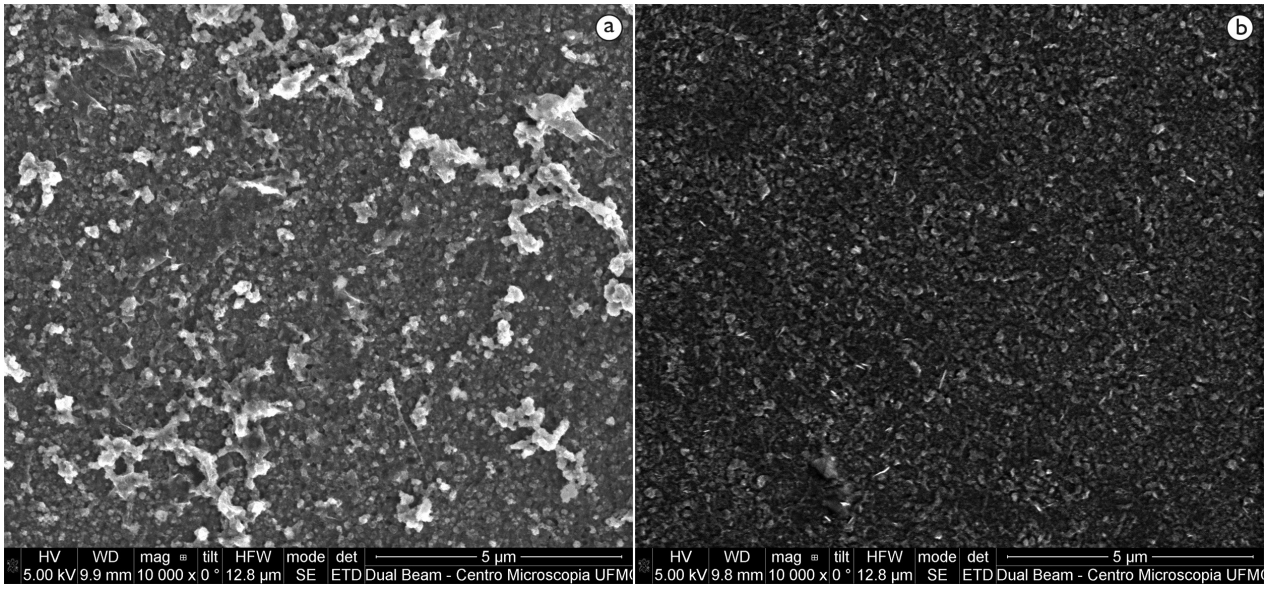

Figure 2. (a) Micrograph of the oxidized steel after immersion in condensed solution (b) Rupture of the inner oxidized layer of the oxidized steel after immersion in condensed solution.

After 240 h of oxidation, the sample oxidized without immersion in condensed solution showed a homogeneous protective film (Figure 4b). Figure 4a shows the surface of the steel sample oxidized after immersion in condensed solution.

EDS analysis on the surface of the AISI 409 steel sample oxidized for 240 hours at 300°C after immersion in condensed solution shows the presence of carbon, iron, silicon, aluminum, oxygen, sodium, calcium, sulfur and chromium (Figure 5). Sulfur can be originated from the condensed solution.

The line EDS spectra indicated in Figure 6 of the TOC sample identified the constituents of the broken oxide layer shown in Figure 3a.

The EDS analysis (Figure 7) of the surface of AISI 409 steel oxidized for 240 hours at 300°C without previous immersion in condensed solution shows the presence of chromium, oxygen, iron, sodium, aluminum, and silicon.

4 DISCUSSIONS

During the oxidation process, there was no significant mass change of the samples, also found by Li et al. [6]. It should be noted that the mass gain of the sample oxidized after immersion in condensed solution was two orders of magnitude higher than the mass gain of the sample oxidized without immersion in condensed solution. This result can

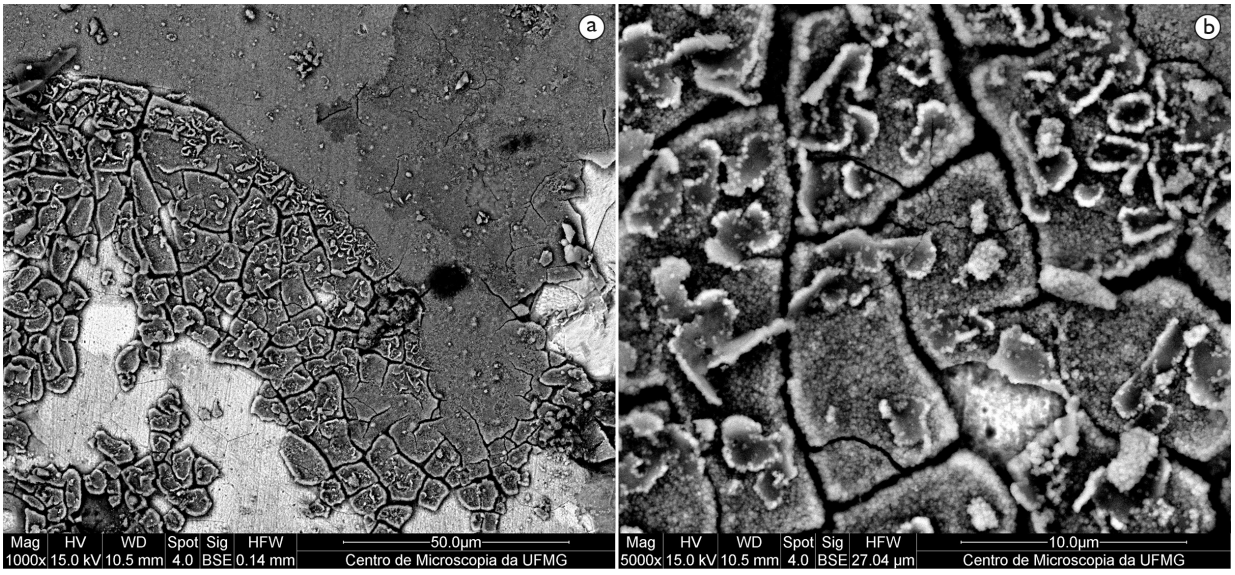

Figure 3. (a) Micrograph of the surface of oxidized steel after immersion in condensed solution, showing crevices at the grain boundaries (b) Detail of rupture of the oxide film at the grain boundaries.

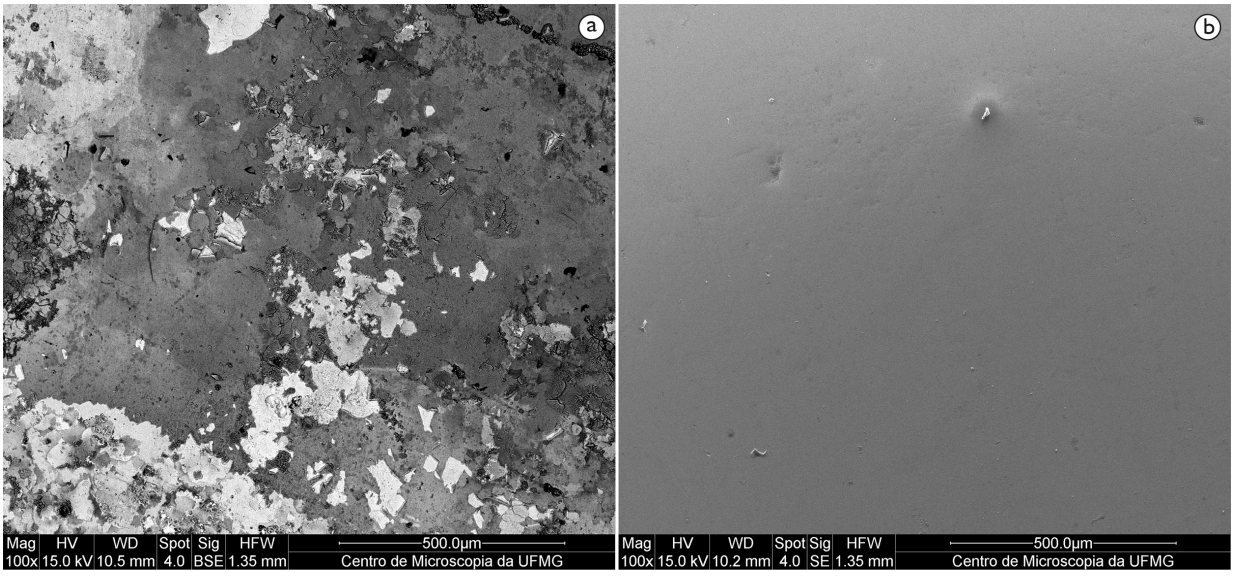

Figure 4. (a) Micrograph of the surface of the steel sample oxidized for 240 hours after immersion in condensed solution. (b) Micrograph of the surface of the steel sample oxidized for 240 hours without previous immersion in condensed solution.

be attributed to the oxide film of the sample oxidized after immersion in condensed solution is not continuous, occurring rupture of the oxide in the grain boundary region. These failures produced a higher consumption of metal to regenerate the oxide layer. The sulfate ions in condensed solution can oxidize generating sulfide ions and HS^- ions, very aggressive to steel. The production of iron sulfides is detrimental to the passive layer. Wang and He [10] reported

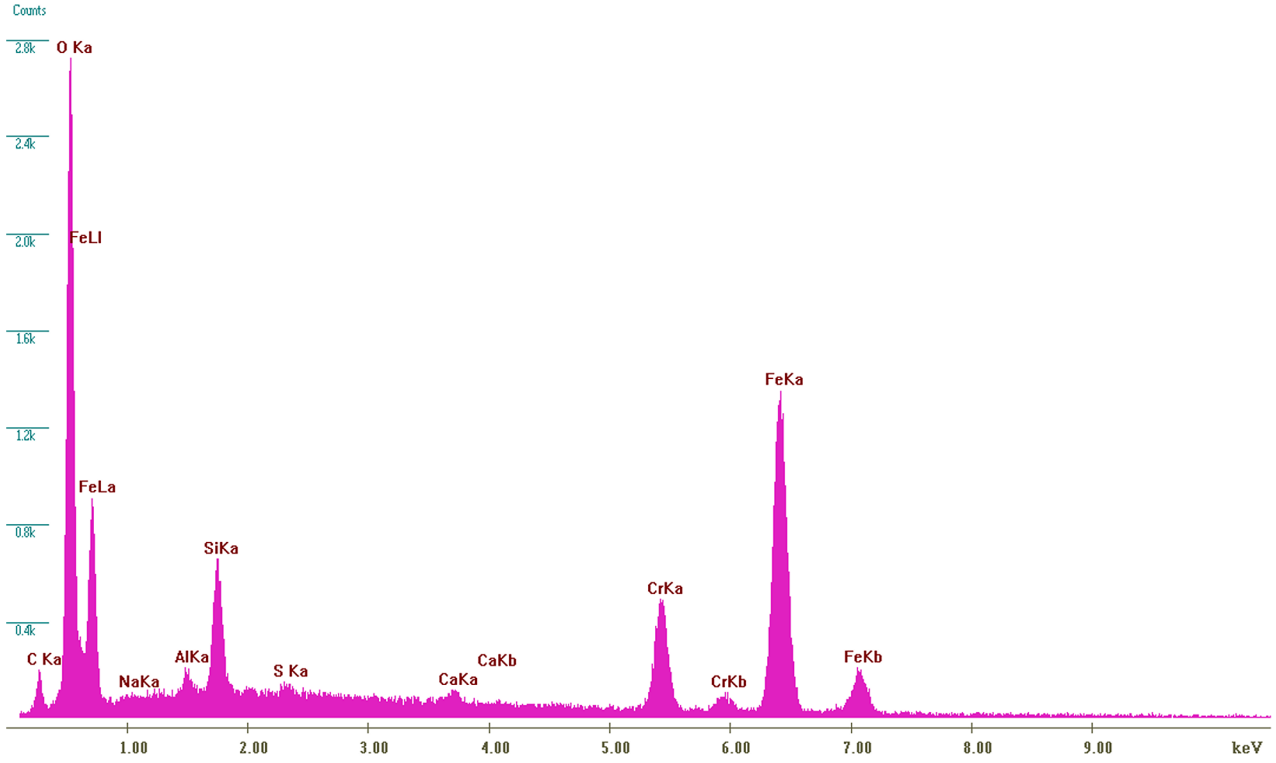

Figure 5. EDS analysis of the oxide film on the surface of AISI 409 steel oxidized in synthetic air for 240 hours at 300°C.

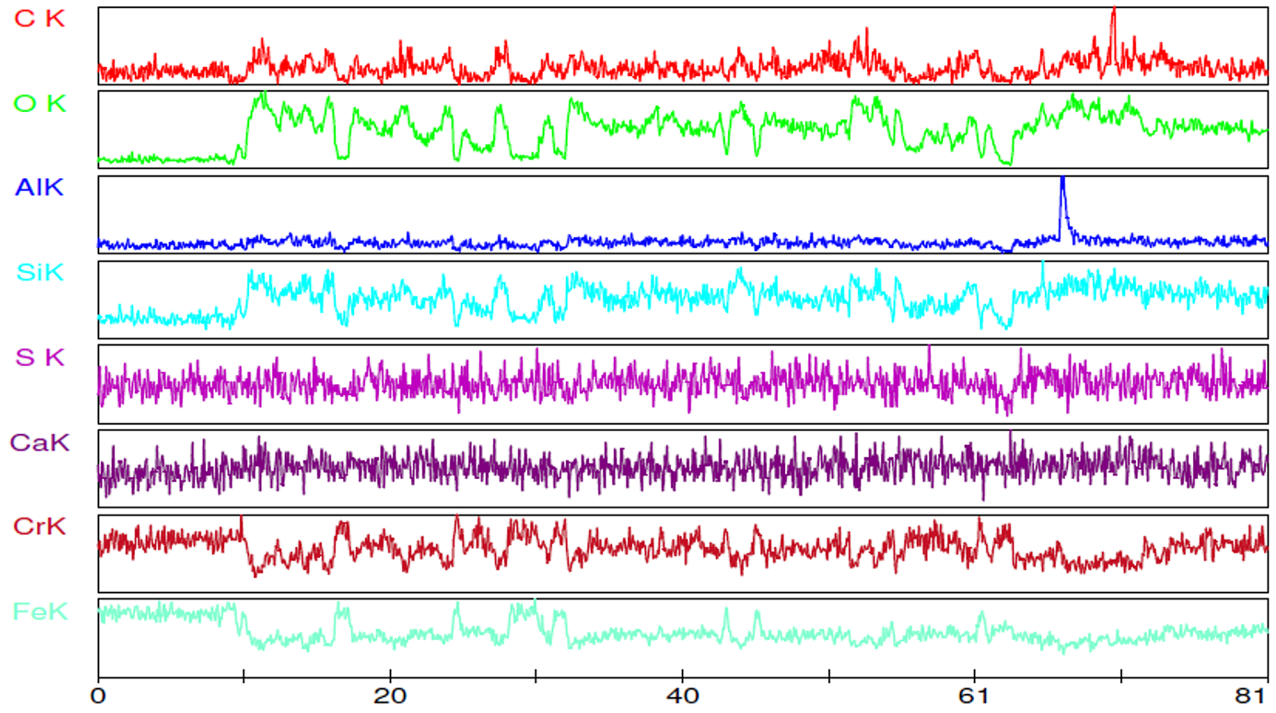

Figure 6. EDS analysis of the constituents of the oxide layer of the TOC sample.

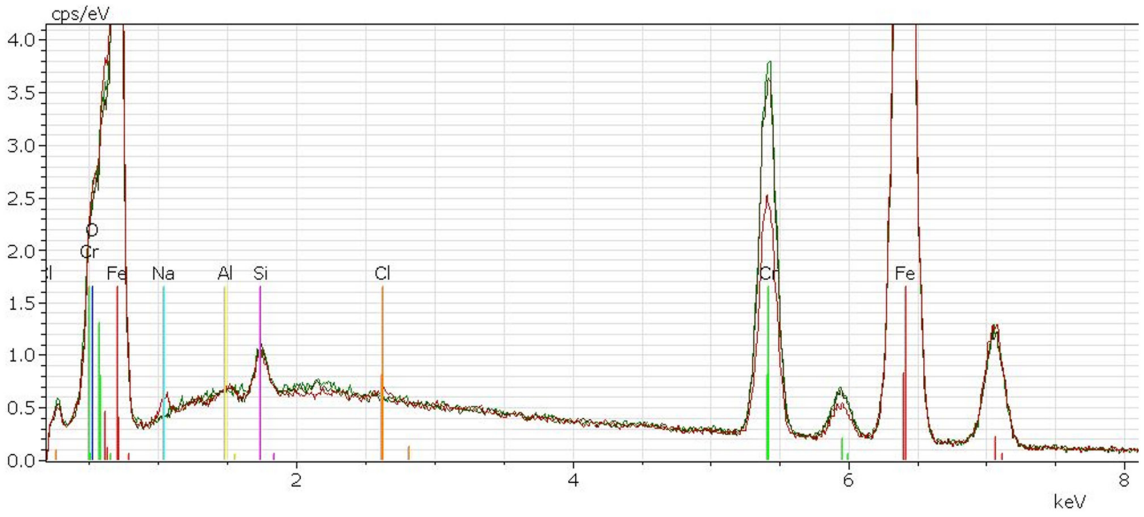

Figure 7. EDS analysis of the oxide layer on the surface of AISI 409 steel oxidized in synthetic air at 300°C for 240 hours without previous immersion in condensed solution.

that sulfidation of sulfate ions accelerates oxidation of AISI 409 steel. The surface color of the samples changed during the oxidation [7].

The fast oxide growth on the surface of stainless steel is explained as a consequence of oxygen vacancies in the oxide film due to the chloride content [11]. As the chloride concentration increases, the rate of vacancies creation increases. The base metal migrates tending to occupy and to eliminate the vacancies. The concentration of the metallic vacancies depends on the rate of creation and elimination of vacancies. If the rate of vacancy creation is higher than the rate of vacancy elimination, the oxide film loses cohesion and suffers localized disruptions [6], as it occurs on the surface of the TOC sample.

The AISI 409 steel stabilized with titanium showed failure of the oxide film after 240 hours of oxidation. The steel used by Li et al. [6] and Cunto [7] did not show the failure of the passive film, but the steel was stabilized by titanium and niobium.

The oxidation of AISI 409 steel could certainly induce high compression stress in adherent oxide film and hence tensile stress in the underlying metal substrate. Li et al. [6] state that these thermal stresses are the result of different thermal expansion coefficients between the metal and film. The aforementioned factors lead to the cracks and even fragmentation of the oxide film during cyclic heating and cooling process.

EDS analysis shows the presence of sulfur on the surface of the AISI 409 steel oxidized after immersion in condensed solution, which is in the form of sulfate or sulfide. Sato and Tanouse [12] reported that the condensed ions are almost completely evaporated, except for minor amounts of ions SO_4^{2-} at 300°C. Chromium and iron sulfides can form in the oxide layer of AISI 409 steel oxidized after immersion in condensed solution. Sulfides can also form at the metal/oxide interface during cyclic tests. The sulfidation of sulfate ions is one of the main factors responsible for accelerating oxidation of the AISI 409 steel [10].

5 CONCLUSIONS

The AISI 409 steel oxidized for 240 hours at 300°C after immersion in condensed solution showed failure of the oxide film, and the steel oxidized without previous immersion in the condensed solution showed a homogeneous oxide film after oxidation with no visible ruptures.

EDS analysis of the oxidized surface of AISI 409 steel after immersion in condensed solution identified the presence of sulfur in the oxide layer.

The mass gain of the sample oxidized for 240 hours without previous immersion in condensed solution was $4.58\ 10^{-5}$ g.cm^{-2}, and the mass gain of the sample oxidized after immersion in condensed solution was $2.21\ 10^{-3}$ g.cm^{-2}.

Acknowledgements

The authors acknowledge the IFPI, UEMA, Fapema, CNPq, Wesller Schmidtand, Breno Barbosa Moreira, Dr John Frank di Fiore for English revision, and the Microscopy Center of Federal University of Minas Gerais.

REFERENCES

1 Palcut M, Mikkelsen L, Neufeld K, Chen M, Knibbe R, Hendriksen PV. Corrosion stability of ferritic stainless steels for solid oxide electrolyser cell interconnects. Corrosion Science. 2010;52(10):3309-3320. http://dx.doi.org/10.1016/j.corsci.2010.06.006.

2 Hultquist G, Leygraf C. Selective oxidation of a ferritic stainless steel and its influence on resistance to crevice corrosion initiation. Corrosion Science. 1981;21(6):401-408. http://dx.doi.org/10.1016/0010-938X(81)90038-X.

3 Phaniraj MP, Kim DI, Cho YW. Effect of grain boundary characteristics on the oxidation behavior of ferritic stainless steel. Corrosion Science. 2011;53(12):4124-4130. http://dx.doi.org/10.1016/j.corsci.2011.08.020.

4 Srisrual A, Coindeau S, Galerie A, Petit JP, Wouters Y. Identification by photoelectrochemistry of oxide phases grown during the initial stages of thermal oxidation of AISI 441 ferritic stainless steel in air or in water vapour. Corrosion Science. 2009;51(3):562-568. http://dx.doi.org/10.1016/j.corsci.2008.12.002.

5 Issartel J, Martoia S, Charlot F, Parry V, Parry G, Estevez R, et al. High temperature behavior of the metal/oxide interface of ferritic stainless steels. Corrosion Science. 2012;59:148-156. http://dx.doi.org/10.1016/j.corsci.2012.02.025.

6 Li MC, Wang SD, Ma RY, Han PH, Bi HY. Effect of cyclic oxidation on electrochemical corrosion of type 409 stainless steel in the simulated muffler condensates. Journal of Solid State Electrochemistry. 2012;16(9):3059-3067. http://dx.doi.org/10.1007/s10008-012-1746-z.

7 Cunto JC. Estudo da Resistência à corrosão de aços inoxidáveis para uso na parte fria dos sistemas de exaustão de veículos [Master's thesis]. São Paulo: IPEN; 2005.

8 Hibino AH. Estudo de Tenacidade da Zona Termicamente afetada dos aços inoxidáveis ferríticos UNS S41001 e UNS S41003 [Master's thesis]. Belo Horizonte: UFMG; 2011.

9 Passos ER. Caracterização microestrutural de tubos soldados AISI 409 estabilizado ao titânio: estudo comparativo dos processos TIG e laser [Monograph]. Lorena: USP; 2009.

10 Wang C-J, He TT. Morphological development of subscale formation in Fe-Cr-(Ni) alloys with chloride and sulfates coating. Oxidation of Metals. 2002;58(3/4):415-437. http://dx.doi.org/10.1023/A:1020119107724.

11 NucleoInox. São Paulo; 2009. [cited 2009]. Available at: www.nucleoinox.org.br

12 Sato E, Tanouse T. Present and future trends of materials steel. Japan: NSSMC; 1995. p. 13-19. (Nippon Steel Technical Report, 64).

Received: 28 May 2014
Accepted: 28 May 2015